SEASONAL AND GEOGRAPHICAL VARIABILITY OF THE SURFACE WIND AND STRESS RESPONSES TO SST OVER MID-LATITUDES

Larry O'Neill[1],

Dudley Chelton[1], Steve Esbensen[1], and Tracy Haack[2]

[1]*College of Earth, Ocean, and Atmospheric Sciences, Oregon State University*

[2]*Naval Research Laboratory, Monterey, CA*

- Both surface stress and ENW respond linearly to SST on the oceanic mesoscale. Why?
- Relate spatially high-pass filtered surface wind stress perturbations to those of the ENW, and apply this relationship to wind-SST coupling observed from the QuikSCAT scatterometer and AMSR-E SST
- The stress response to SST is directly proportional to the ENW response with a proportionality factor containing the ambient large-scale ENW
- Variability of the large-scale ENW accounts for variability of the stress response to SST relative to the ENW response

Introduction

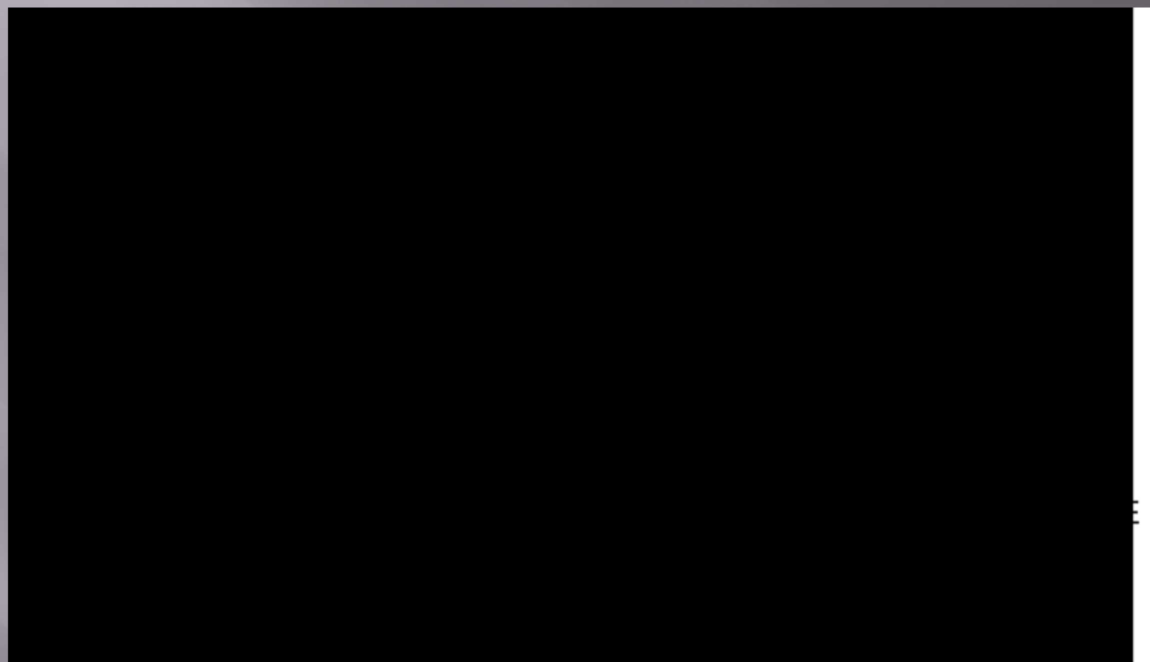

- 7-year average from June 2002-May 2009
- Spatially high-pass filtered wind (colors) and SST (contours) retain wavelengths shorter than 20° lon x 10° lat
- ENW = 10-m equivalent neutral wind speed

What is our current understanding for what is responsible for surface wind responses to mesoscale SST perturbations?

- On weekly and longer timescales, surface neutral wind response due primarily from a response of the actual surface winds to SST (i.e., O'Neill 2012 JCLI; Jim Edson's next talk)
- At least 100 papers published on this subject with evidence of a variety of mechanisms. Essentially, the surface wind response to SST is a manifestation of the response of the entire MABL to spatially-varying surface heating perturbations induced by SST fronts.
- Dynamically, these mechanisms can be summarized fairly as:
  - Adjustments of the vertical turbulent stress divergence, including vertical momentum transfer from aloft to the surface, boundary layer height adjustments in an equilibrium regime, and surface drag modification
  - Pressure adjustments from thermodynamic control of a variable depth MABL, such that lower pressure is found over warmer water and higher pressure over cooler water (includes "sea-breeze" type circulations)
  - SST-induced baroclinic pressure gradients, which can modify the vertical wind speed and directional shear and hence modify vertical mixing depending on orientation of MABL thermal wind vector relative to surface flow
  - Sfc drag perturbations which counteract SST-induced pressure gradient driven flow
- Imbalances between these various mechanisms produce parcel accelerations that lead to stronger winds over warmer water and weaker winds over cooler water

Agulhas Return Current

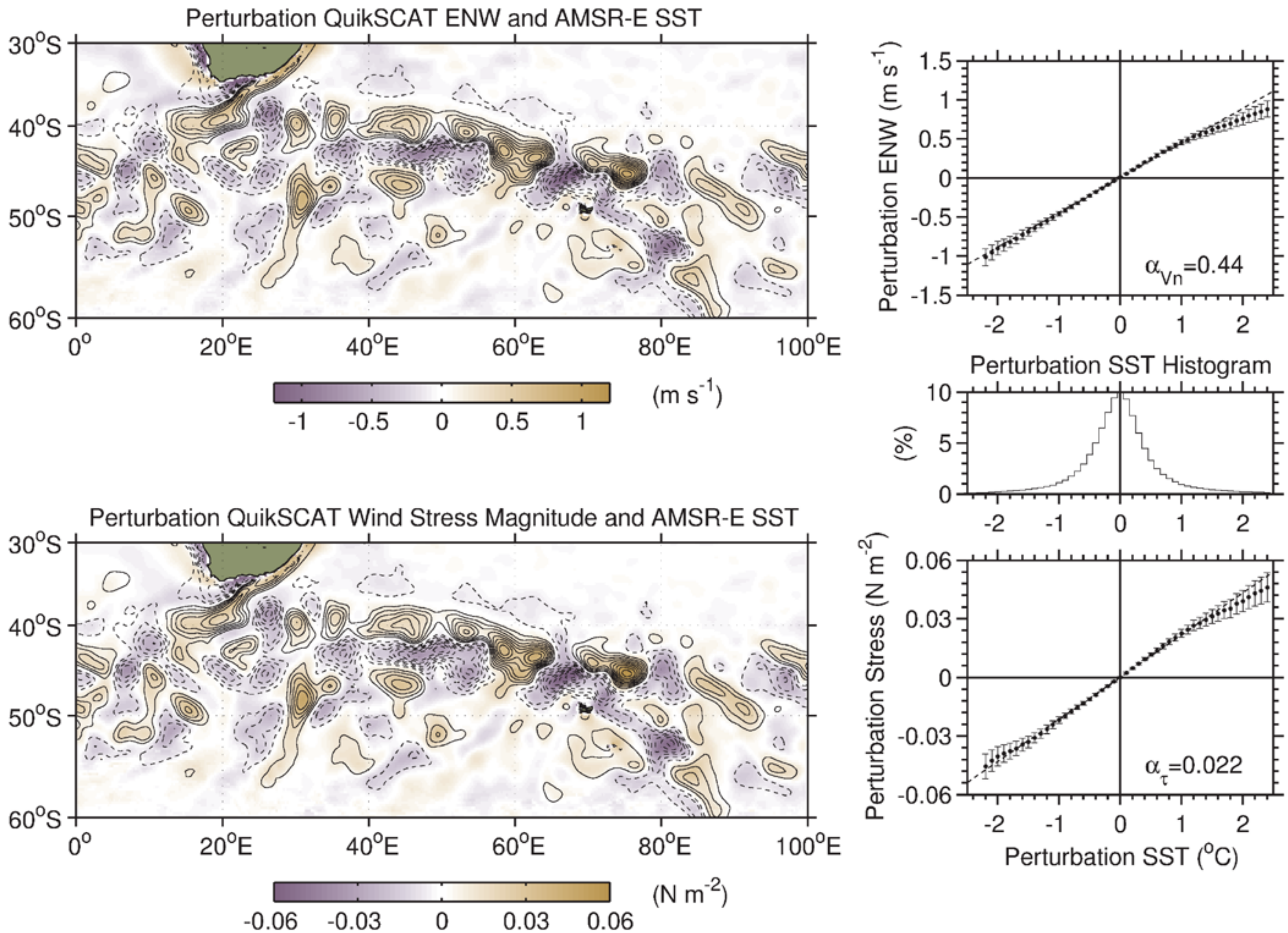

$$\overline{V_n}' \approx \alpha_{vn}\overline{T_s}',$$

$$\alpha_{vn} = \frac{\partial \overline{V_n}'}{\partial \overline{T_s}'}$$

$$\overline{|\tau|}' \approx \alpha_{\tau}\overline{T_s}'$$

$$\alpha_{\tau} = \frac{\partial \overline{|\tau|}'}{\partial \overline{T_s}'}$$

- 7-year average from June 2002-May 2009
- Binned averages computed from monthly-averaged wind and SST fields
- Even though stress is a nonlinear function of ENW, both the stress and ENW respond linearly to SST on the oceanic mesoscale

How is surface stress estimated from scatterometer ENW?

$$|\tau| = \rho_0 C_{d10n} V_n^2,$$

$$C_{d10n} = \frac{a_0}{V_n} + b_0 + c_0 V_n,$$

$$\boxed{|\tau| = \rho_0 \left(a_0 V_n + b_0 V_n^2 + c_0 V_n^3 \right) .}$$

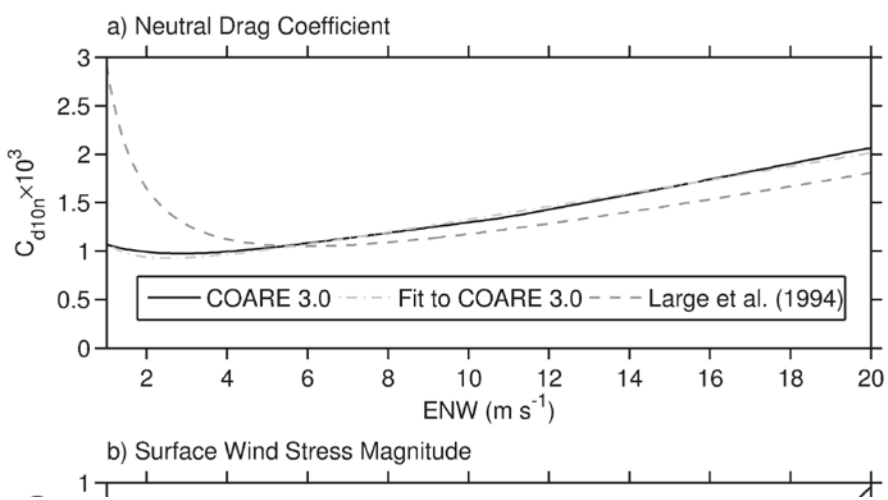

North Atlantic

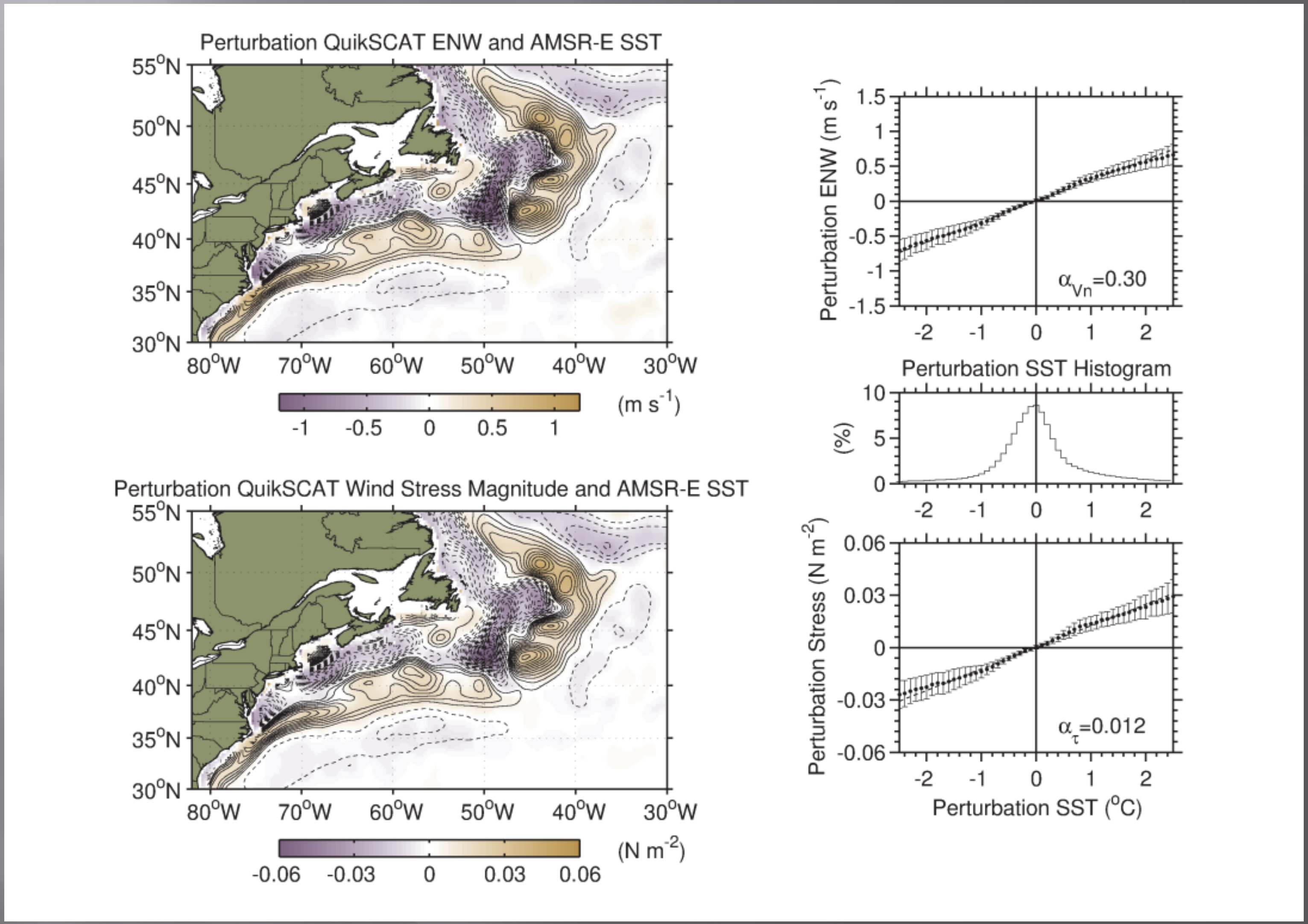

South Atlantic

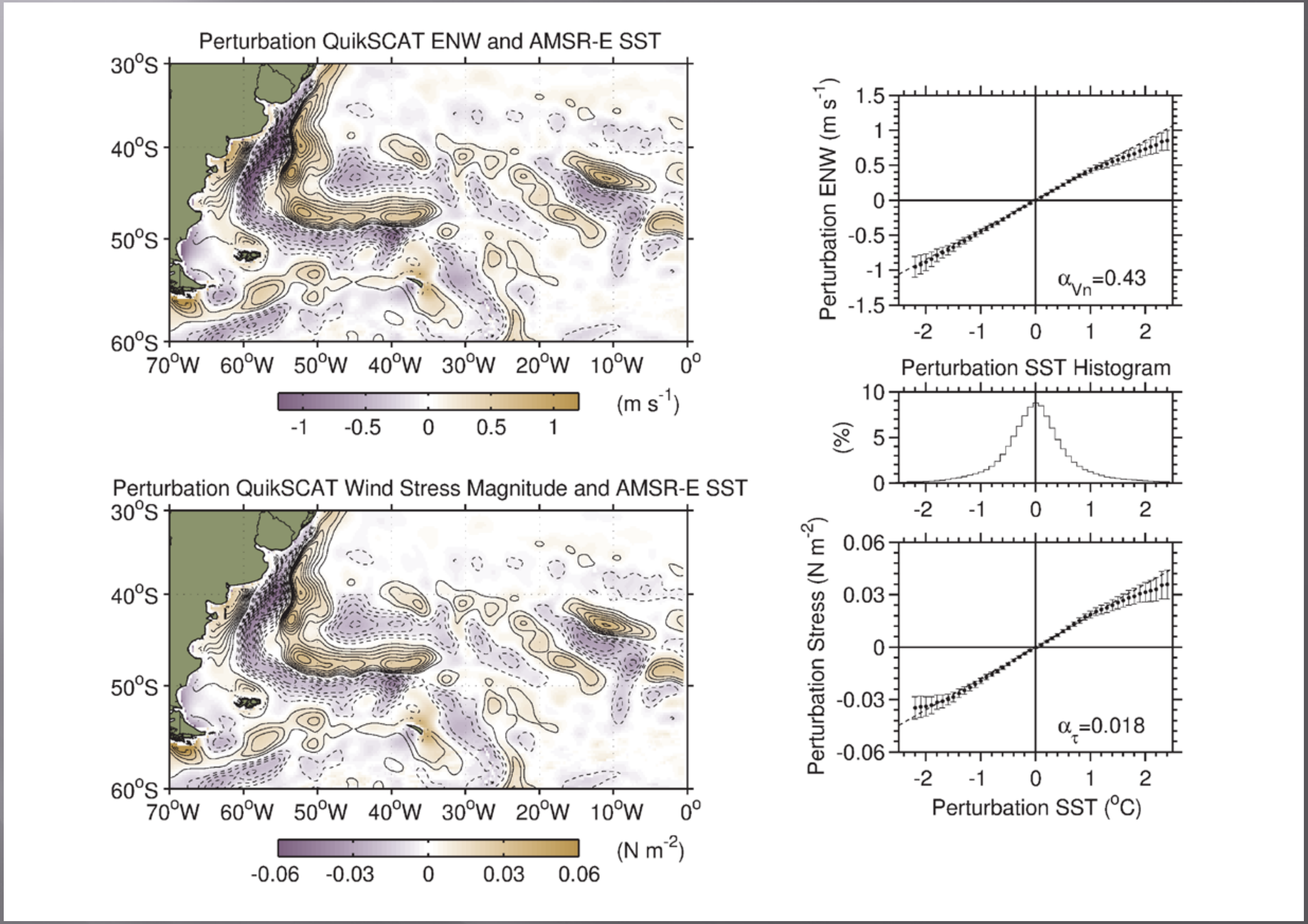

Kuroshio Extension

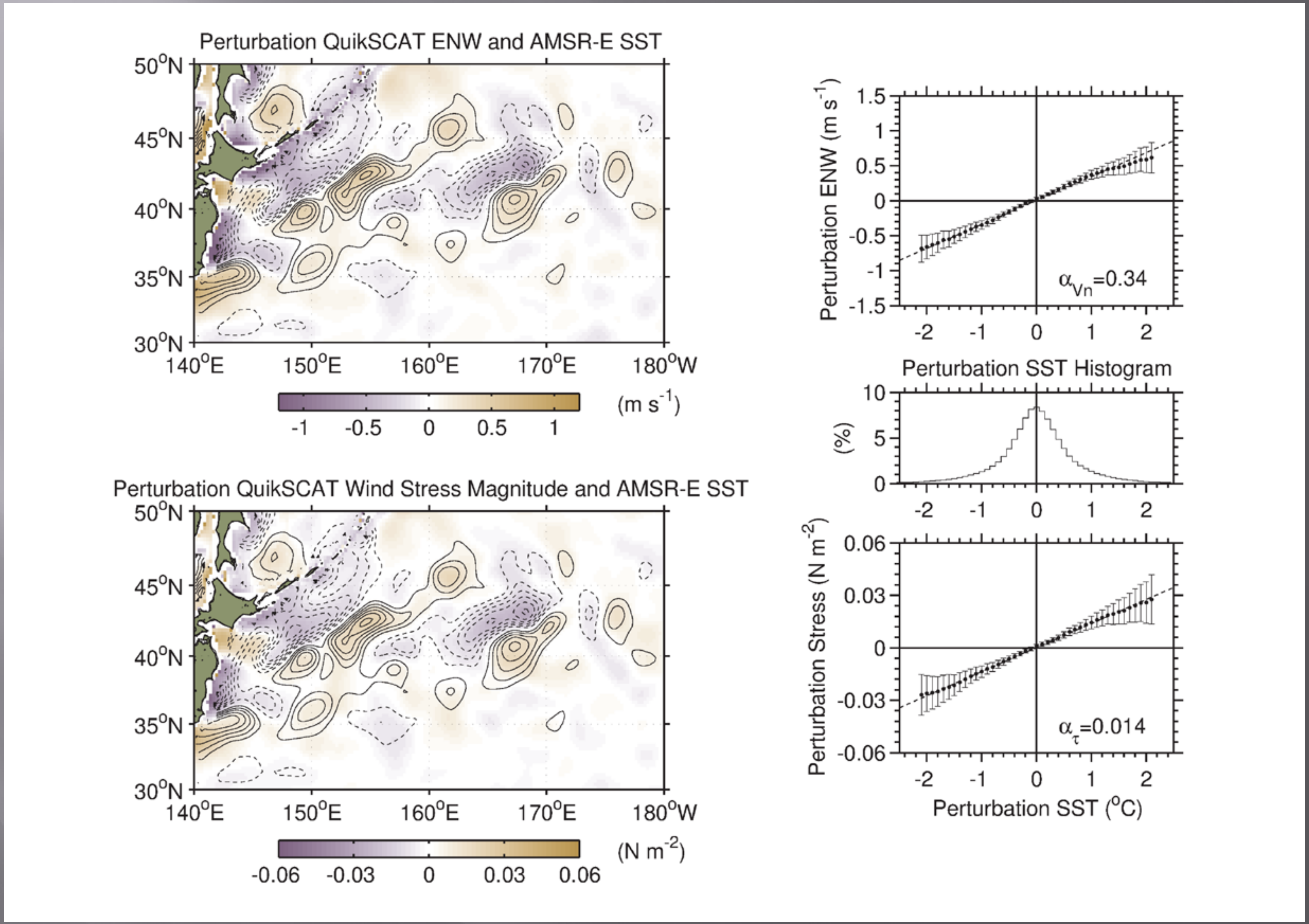

Summary statistics for 7 years of QuikSCAT and AMSR-E observations

Region	Corr. Coef. with $\overline{T_s}'$		$\alpha_\tau \times 100$	α_{Vn}
	$\overline{\lvert\tau\rvert}'$	$\overline{V_n}'$	N m^{-2} °C^{-1}	m s^{-1} °C^{-1}
Kuroshio	0.45	0.56	1.4 ± 0.2	0.34 ± 0.05
[redacted]				

Stronger stress and ENW responses to SST over Southern Hemisphere compared to Northern Hemisphere

ENW coupling coefficient estimates from various combinations of satellite ENW and SST datasets

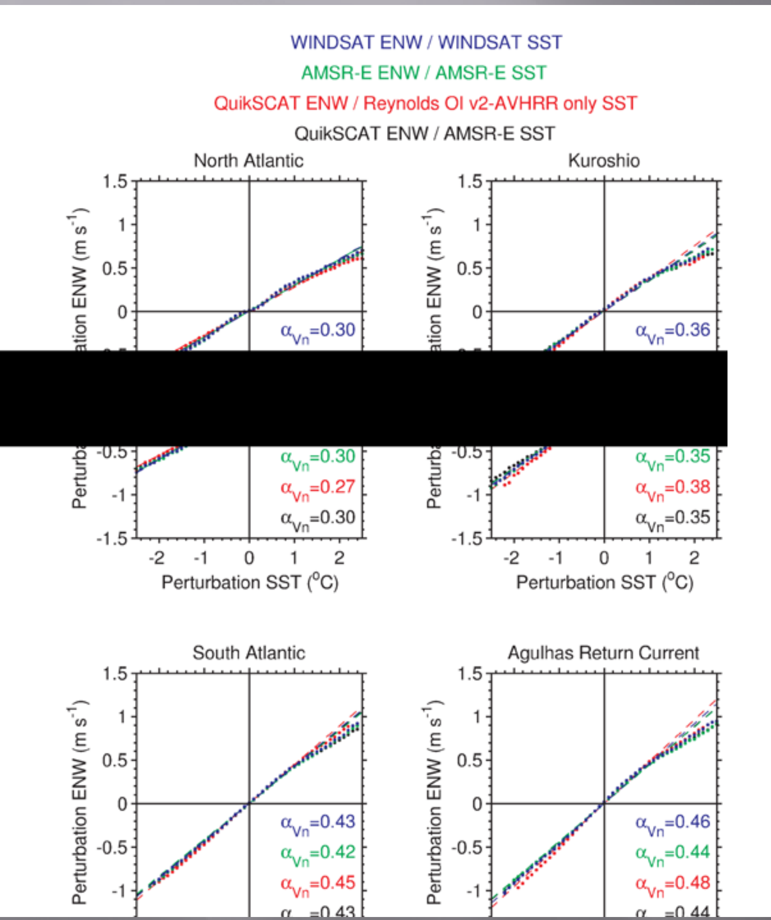

All datasets processed by Remote Sensing Systems

ENW	SST	N. Atlantic	Kuroshio	S. Atlantic	Agulhas
QuikSCAT v4	AMSR-E v7	0.30	0.35	0.43	0.44
QuikSCAT v3	AMSR-E v5	0.32	0.37	0.44	0.47
WindSat v7	WindSat v7	0.30	0.36	0.43	0.46
AMSR-E v7	AMSR-E v7	0.30	0.35	0.42	0.44
QuikSCAT v4	Reynolds OI-v2	0.27	0.38	0.45	0.48

Only <~10% difference in ENW coupling coefficient estimates between different combinations of datasets over all regions (QSCAT v4 and AMSR-E v7 used throughout this analysis)

Time series of ENW coupling coefficients from various satellite dataset combinations

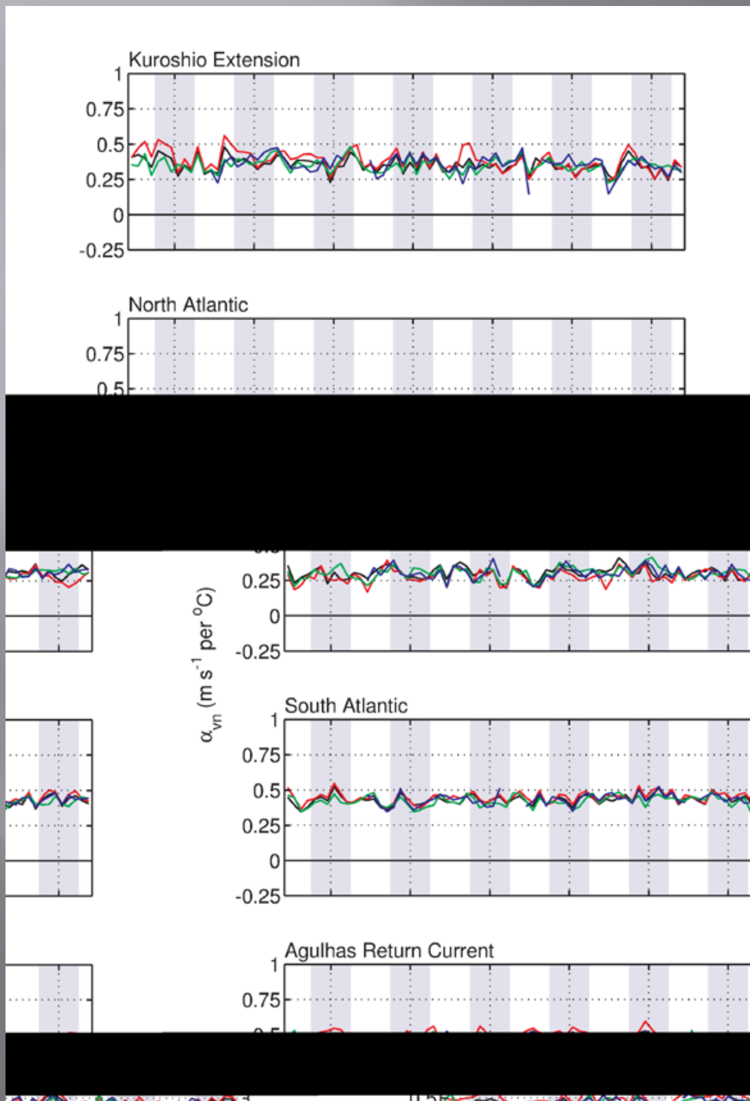

- Different color curves represent a different satellite dataset combination
- No significant temporal differences in ENW coupling coefficients between dataset combinations
- No significant temporal variability (particularly seasonal or interannual) evident in ENW responses to SST

Time series of stress and ENW coupling coefficients

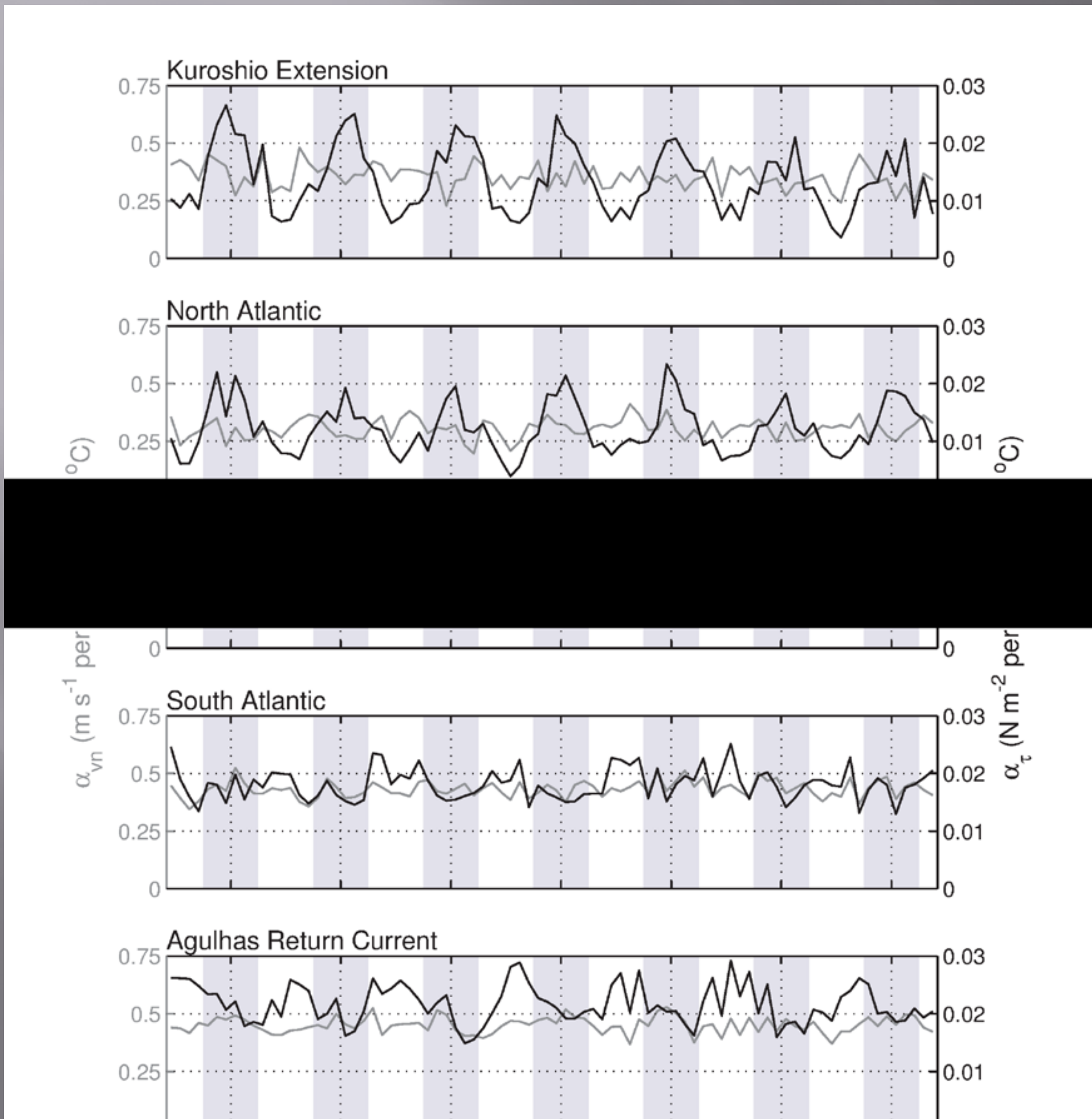

- ENW coupling coefficients (grey curves) have a relatively small seasonal cycle
- Stress coupling coefficients (black curves) have a large seasonal cycle, with a 50-300% stronger stress response during winter compared to summer

Global maps of coupling coefficients

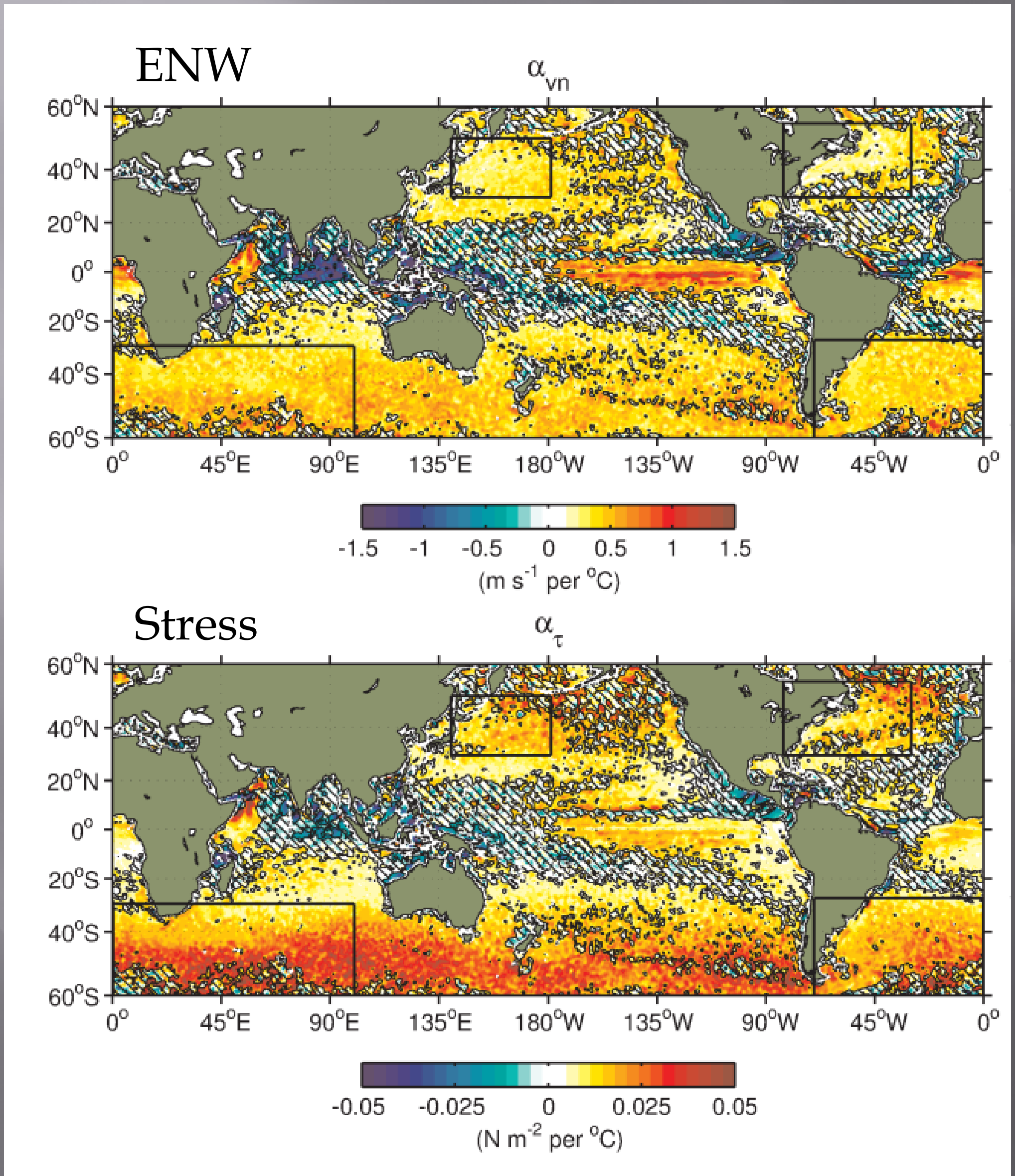

- QuikSCAT v4 ENW and AMSR-E v7
- Cross-hatched areas are not statistically significant
- ENW response is more uniform while the stress response is largest in mid-latitude westerly wind belts and weakest in weak wind regimes associated with subtropical highs

Relating the stress and ENW responses to SST on the ocean mesoscale

$$V_n = \overline{\widetilde{V_n}} + \overline{V_n}' + \widetilde{V_n}^* + V_n'^*,$$

- $\overline{\widetilde{V_n}}$ is the monthly-averaged, spatially low-pass filtered ENW;
- $\overline{V_n}'$ is the monthly-averaged, spatially high-pass filtered ENW;
- $\widetilde{V_n}^*$ is the time-varying (on sub-monthly time-scales), spatially low-pass filtered ENW;
- and $V_n'^*$ is the time-varying, spatially high-pass filtered ENW.

$$\overline{|\tau|}' \approx \rho_0 \left(a_0 + 2b_0 \overline{\widetilde{V_n}} + 3c_0 \overline{\widetilde{V_n}}^2 \right) \overline{V_n}' + \rho_0 \left[\left(b_0 + 3c_0 \overline{V_n} \right) \overline{V_n^{*2}} + c_0 \overline{V_n^{*3}} \right]'.$$

Details in O'Neill et al. (2012, JCLI In press)

Relating the stress and ENW responses to SST on the ocean mesoscale

$$\overline{|\tau|}' \approx \rho_0 \left(a_0 + 2b_0 \widetilde{\overline{V_n}} + 3c_0 \widetilde{\overline{V_n}}^2 \right) \overline{V_n}' + \rho_0 \left[\left(b_0 + 3c_0 \overline{V_n} \right) \overline{V_n^{*2}} + c_0 \overline{V_n^{*3}} \right]'.$$

$$\rho_0 \left[\left(b_0 + 3c_0 \overline{V_n} \right) \overline{V_n^{*2}} + c_0 \overline{V_n^{*3}} \right]' \approx \beta_\tau \overline{T_s}'.$$

Perturbation ENW on submonthly timescales are related linearly to monthly-averaged SST, consistent with Sampe and Xie (2007, BAMS); only contributes to <~15% of perturbation stress variability

$$\overline{|\tau|}' \approx \left(\Gamma_n \alpha_{vn} + \beta_\tau \right) \overline{T_s}',$$

$$\boxed{\alpha_\tau \approx \Gamma_n \alpha_{vn} + \beta_\tau.}$$

$$\Gamma_n = \rho_0 \left(a_0 + 2b_0 \widetilde{\overline{V_n}} + 3c_0 \widetilde{\overline{V_n}}^2 \right).$$

Stress response to SST is directly proportional to ENW response to SST multiplied by a factor of the ambient large-scale ENW

Relating ratio of stress and ENW responses to Γ_n

$$\alpha_\tau \approx \Gamma_n \alpha_{vn} + \beta_\tau.$$

$$\Gamma_n \approx \frac{\alpha_\tau - \beta_\tau}{\alpha_{vn}}$$

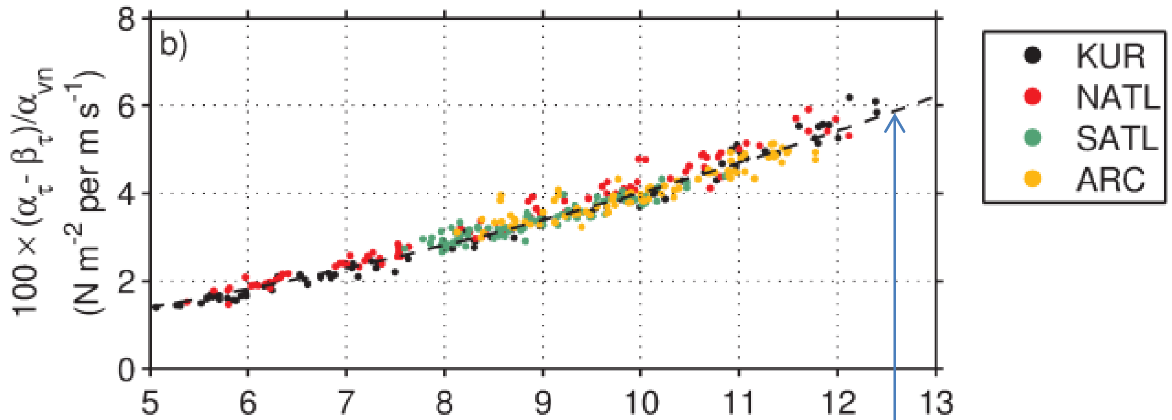

Ambient large-scale ENW (m/s)

$$\Gamma_n = \rho_0 \left(a_0 + 2b_0 \widetilde{\overline{V_n}} + 3c_0 \widetilde{\overline{V_n}}^2 \right).$$

- Each point is from one month for each region during the 84 month period June 2002-May 2009
- Stress relative to the ENW response varies mostly as a function of the ambient large-scale ENW

Summary

- Surface stress and ENW perturbations are both linearly related to SST on the oceanic mesoscale
- Spatially high-pass filtered surface wind stress perturbations are related uniquely to those of the ENW, and the stress response to SST is directly proportional to the ENW response with a proportionality factor containing the ambient large-scale ENW
- Seasonal and geographic variability of the large-scale ENW accounts for seasonal and geographic variations of the stress response to SST relative to the ENW response
- Analogous result for relationship between vector wind stress and ENW derivative fields, although somewhat more complicated than for the simple scalar magnitude cases presented here

Behavior of Γ_n

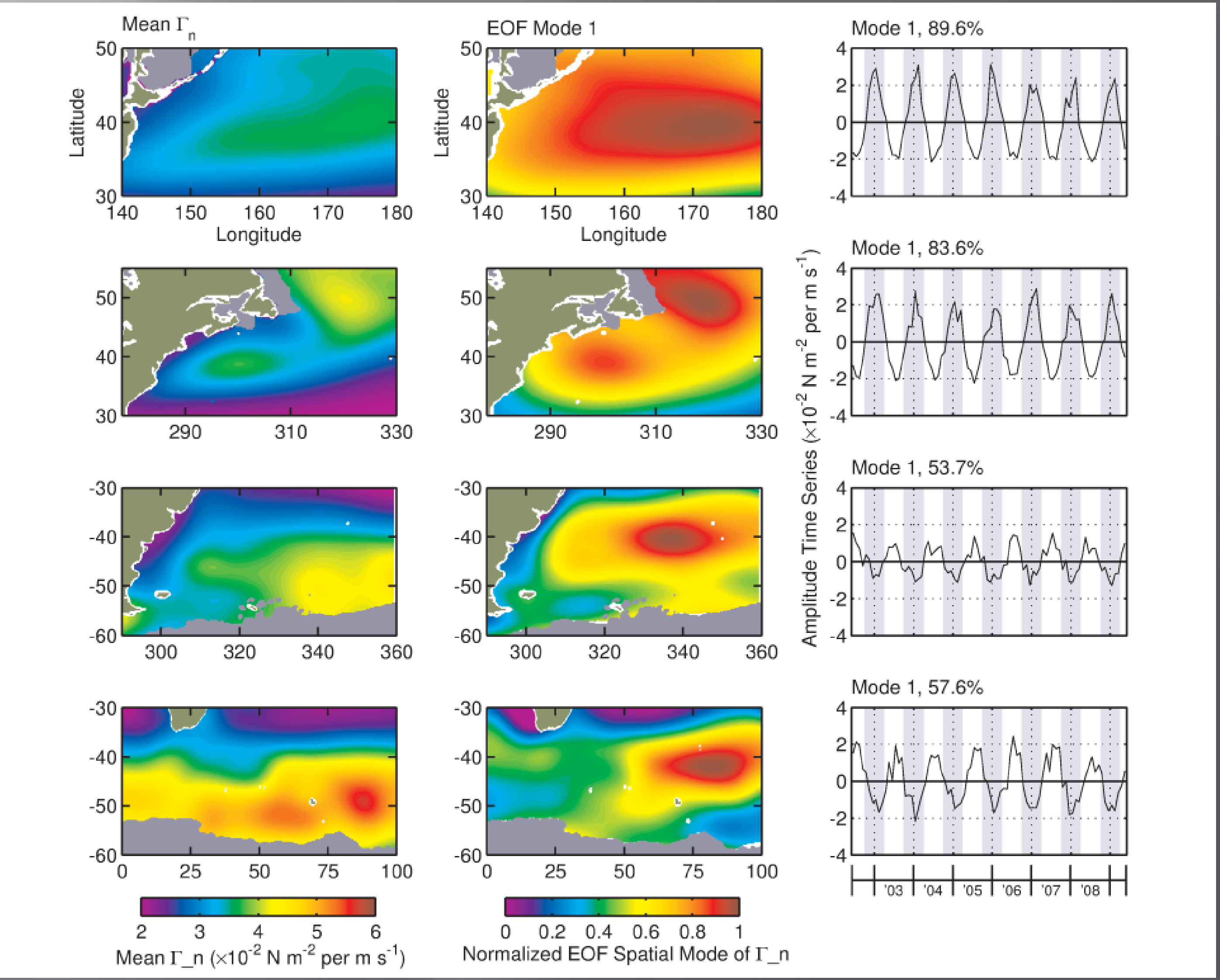

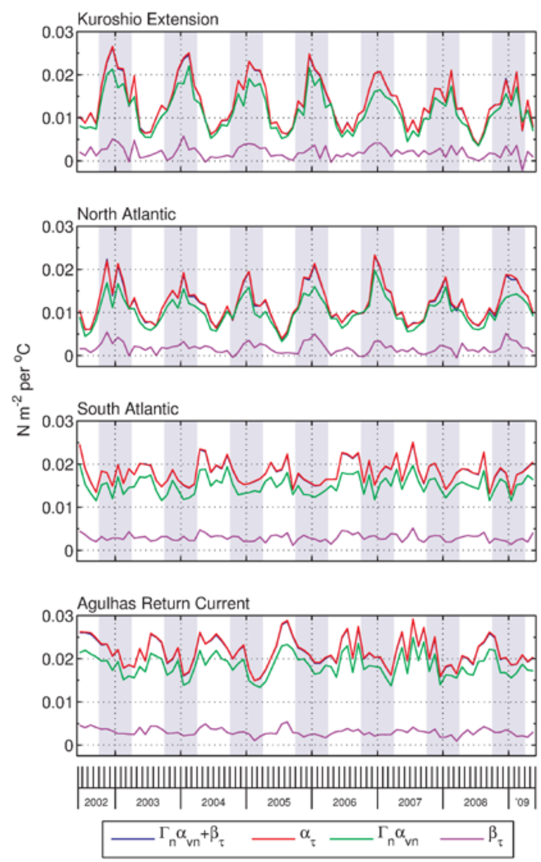

Kuroshio Extension
North Atlantic
South Atlantic
Agulhas Return Current
N m^-2 per °C
0.03
0.02
0.01
0
2002
2003
2004
2005
2006
2007
2008
'09
Γnαvn+βτ
ατ
Γnαvn
βτ

Coupling coefficient as a function of smoothing cutoff wavelengths

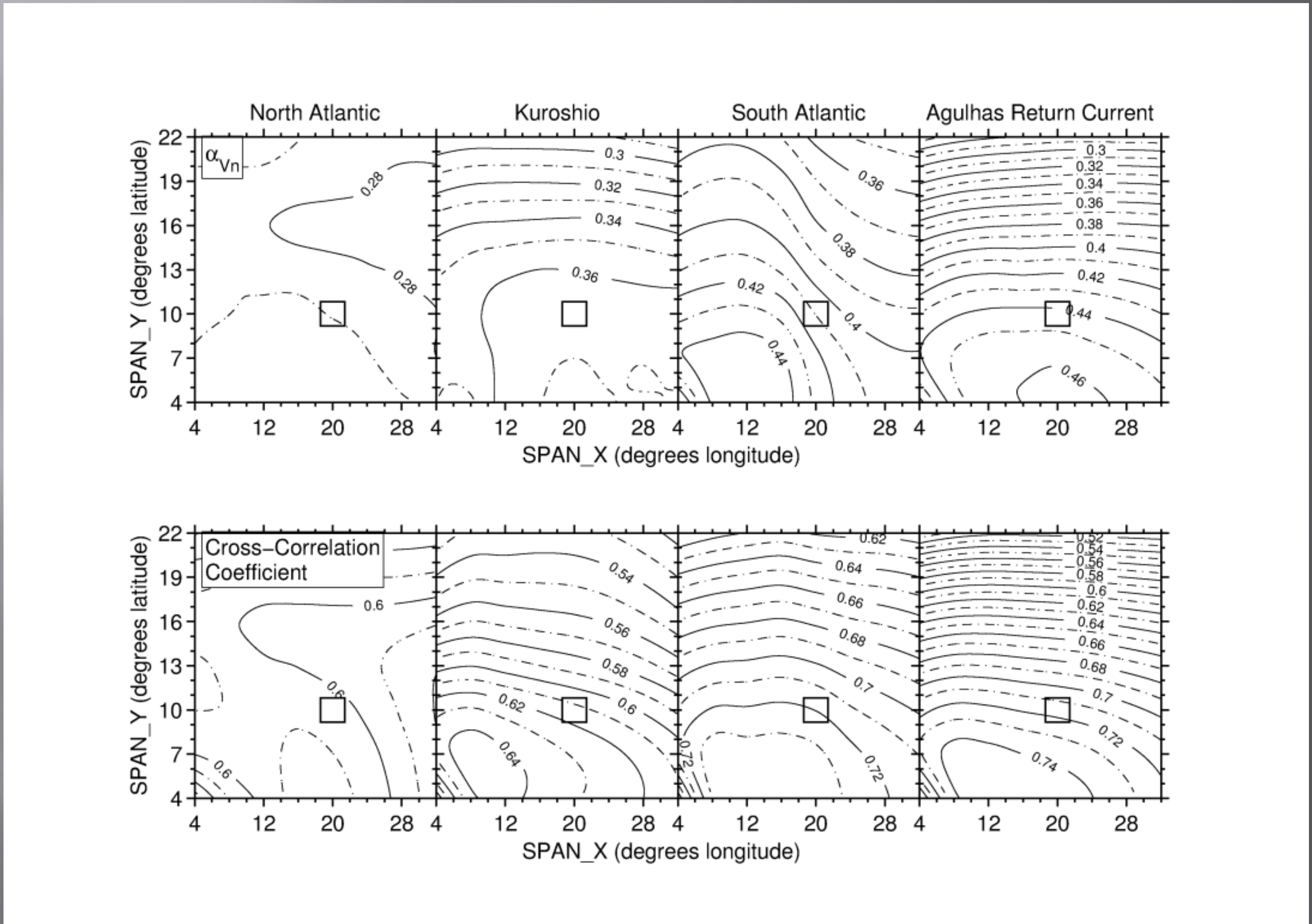

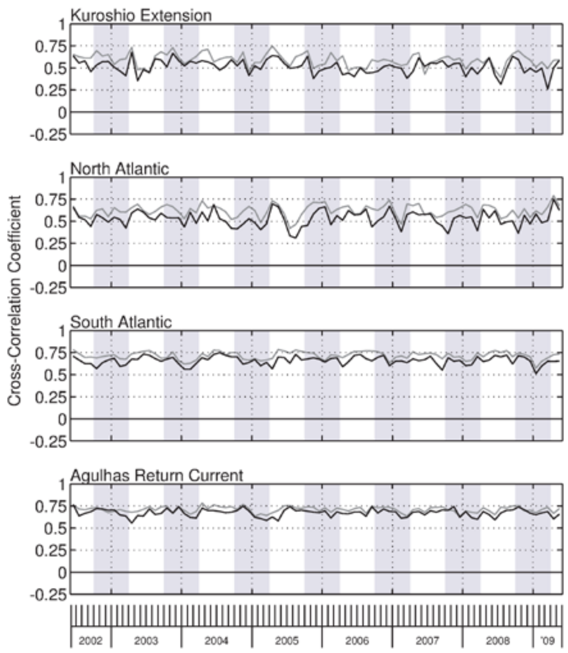
Kuroshio Extension
North Atlantic
South Atlantic
Agulhas Return Current
Cross-Correlation Coefficient
1
0.75
0.5
0.25
0
-0.25
2002
2003
2004
2005
2006
2007
2008
'09

Region	Corr. Coef. with $\overline{T_s}'$ $\overline{\|\tau\|}'$	$\overline{V_n}'$	$\alpha_\tau \times 100$ N m^{-2} °C^{-1}	α_{Vn} m s^{-1} °C^{-1}	α_τ/α_{Vn} $\times 100$	Median ENW m s^{-1}	$\beta_\tau \times 100$ N m^{-2} °C^{-1}
Kuroshio	0.45	0.56	1.4 ± 0.2	0.34 ± 0.05	4.1	8.3	0.19 ± 0.03
North Atlantic	0.50	0.62	1.2 ± 0.2	0.30 ± 0.05	4.0	8.3	0.18 ± 0.03
South Atlantic	0.66	0.72	1.8 ± 0.1	0.43 ± 0.03	4.2	8.9	0.29 ± 0.03
Agulhas	0.67	0.71	2.2 ± 0.1	0.44 ± 0.03	4.9	9.9	0.30 ± 0.02

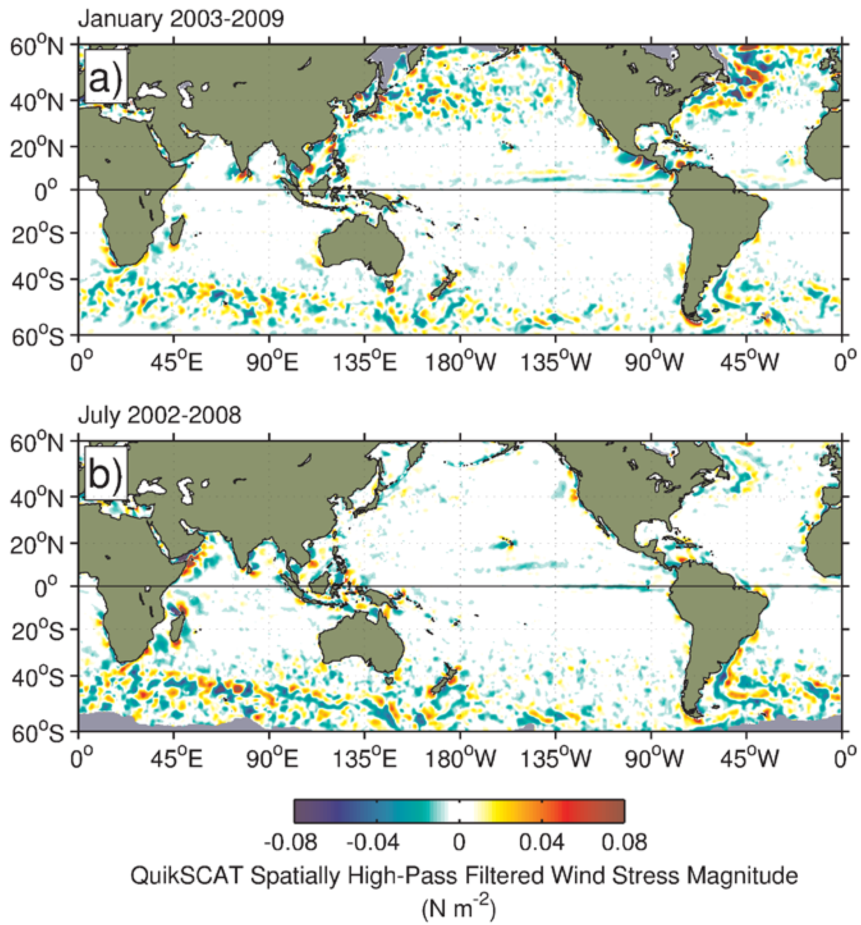
January 2003-2009
a)
60°N
40°N
20°N
0°
20°S
40°S
60°S
0°
45°E
90°E
135°E
180°W
135°W
90°W
45°W
0°
July 2002-2008
b)
-0.08
-0.04
0
0.04
0.08
QuikSCAT Spatially High-Pass Filtered Wind Stress Magnitude
(N m-2)

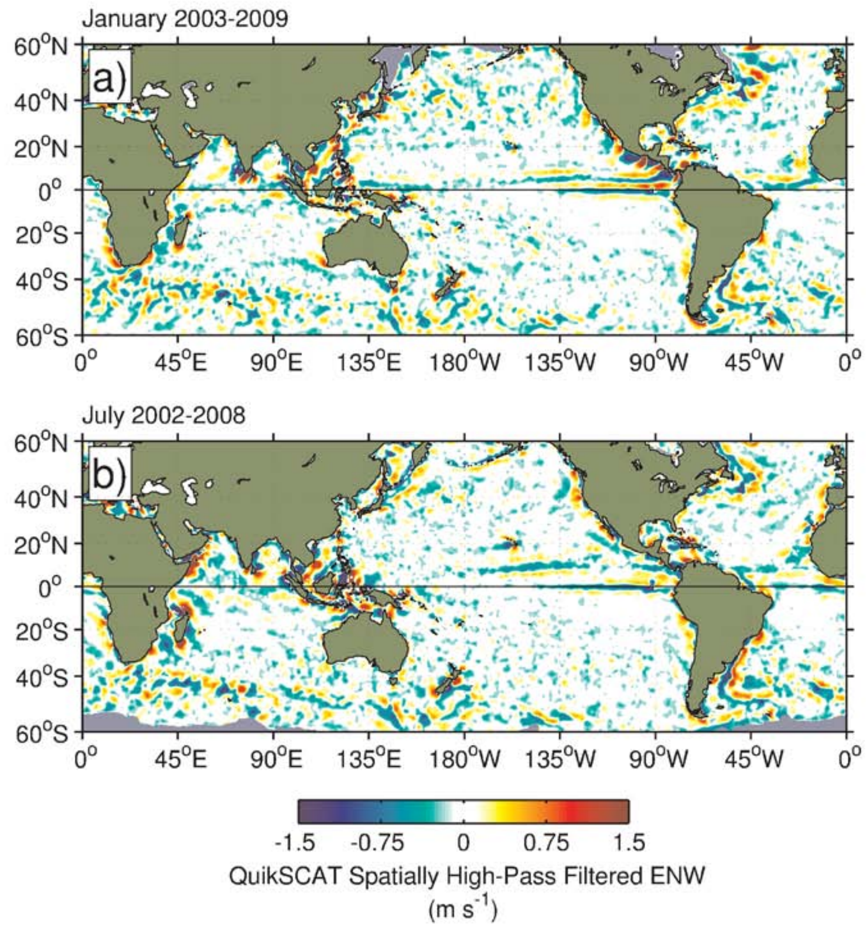
January 2003-2009
a)
July 2002-2008
b)
60°N
40°N
20°N
0°
20°S
40°S
60°S
0°
45°E
90°E
135°E
180°W
135°W
90°W
45°W
0°
-1.5
-0.75
0
0.75
1.5
QuikSCAT Spatially High-Pass Filtered ENW
(m s-1)

$$\alpha_\tau = \frac{\partial \overline{|\tau|}'}{\partial \overline{T_s}'}$$

$$\overline{|\tau|}' \approx \alpha_\tau \overline{T_s}'$$

$$\alpha_{vn} = \frac{\partial \overline{V_n}'}{\partial \overline{T_s}'}$$

$$\overline{V_n}' \approx \alpha_{vn} \overline{T_s}',$$

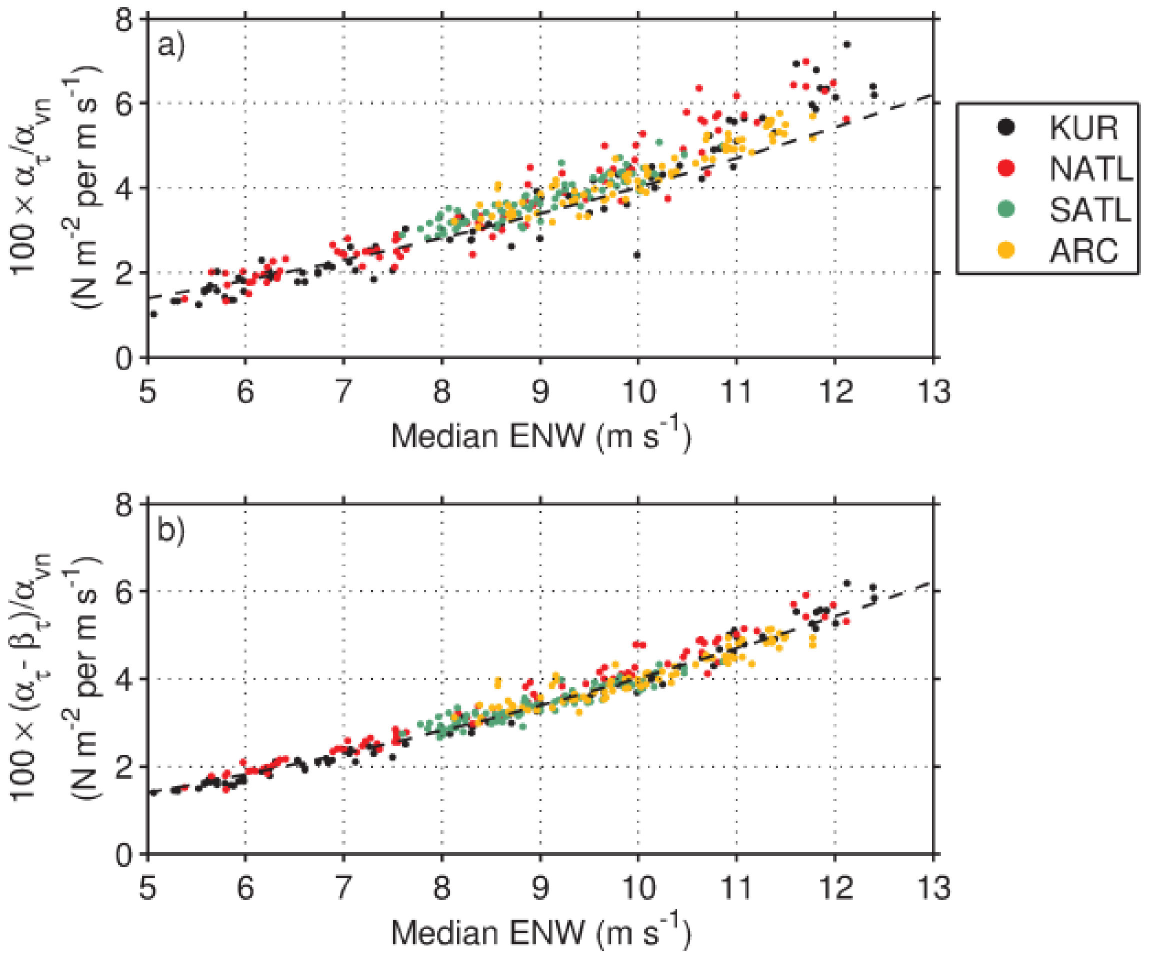
a)
b)
$100 \times \alpha_\tau / \alpha_{vn}$
$(N\ m^{-2}\ per\ m\ s^{-1})$
$100 \times (\alpha_\tau - \beta_\tau) / \alpha_{vn}$
$(N\ m^{-2}\ per\ m\ s^{-1})$
Median ENW $(m\ s^{-1})$
KUR
NATL
SATL
ARC
0
2
4
6
8
5
6
7
8
9
10
11
12
13

Region	Corr. Coef. with $\overline{T_s}'$ $\overline{\lvert\tau\rvert}'$	$\overline{V_n}'$	$\alpha_\tau \times 100$ N m^{-2} °C^{-1}	α_{Vn} m s^{-1} °C^{-1}	α_τ/α_{Vn} $\times100$	Median ENW m s^{-1}	$\beta_\tau \times 100$ N m^{-2} °C^{-1}
Kuroshio	0.45	0.56	1.4 ± 0.2	0.34 ± 0.05	4.1	8.3	0.19 ± 0.03
North Atlantic	0.50	0.62	1.2 ± 0.2	0.30 ± 0.05	4.0	8.3	0.18 ± 0.03
South Atlantic	0.66	0.72	1.8 ± 0.1	0.43 ± 0.03	4.2	8.9	0.29 ± 0.03
Agulhas	0.67	0.71	2.2 ± 0.1	0.44 ± 0.03	4.9	9.9	0.30 ± 0.02